INSTITUTE OF PHYSICS PUBLISHING PHYSICS IN MEDICINE AND BIOLOGY

Phys. Med. Biol. **49** (2004) 5073–5086 PII: S0031-9155(04)84586-X

High-resolution electroencephalogram (EEG) mapping: scalp charge layer

Dezhong Yao[1,4], ZhongKe Yin[2], XiangHong Tang[3], Lars Arendt-Nielsen[4] and Andrew C N Chen[4]

[1] School of Life Science and Technology, University of Electronic Science and Technology of China, Chengdu 610054, People's Republic of China
[2] School of Computer & Communications Engineering, Southwest Jiaotong University, Chengdu 610031, People's Republic of China
[3] School of Communications, Hangzhou Dianzi University, Hangzhou 310012, People's Republic of China
[4] Human Brain Mapping and Cortical Imaging Laboratory, Centre for Sensory Motor Interaction, Aalborg University, Fredrik Bajers Vej 7D3, Aalborg 9220, Denmark

E-mail: dyao@uestc.edu.cn

Received 1 August 2004, in final form 20 September 2004
Published 25 October 2004
Online at stacks.iop.org/PMB/49/5073
doi:10.1088/0031-9155/49/22/004

Abstract

The neural electrical signal related to the human brain function is one of the tracks to understanding ourselves. Various electroencephalogram imaging techniques have been developed to reveal spatial information on neural activities in the brain from scalp recordings, such as Laplacian, equivalent source layer and potential. Physically, these methods may be classified into two categories: scalp surface or cortical surface based techniques. In this work, the focus is on the scalp surface based equivalent charge layer (ECL), with a comparison to the scalp potential with different references and scalp Laplacian (SL). The contents include theoretical analysis and numeric evaluation of simulated data and real alpha (8–12 Hz) data. The results confirm the fact that SL and ECL are of higher spatial resolution than various scalp potential maps, and for SL and ECL, SL is of higher resolution but more sensitive to noise.

(Some figures in this article are in colour only in the electronic version)

1. Introduction

Though it is a widely utilized non-invasive technique for diagnosing or exploring the function of the nervous system with regard to normal or pathological conditions, scalp electroencephalogram (EEG) recordings suffer from spatial smearing distortion of head volume conductor and the effect of non-neutral reference (Nunez *et al* 1994, Yao 2001a). The

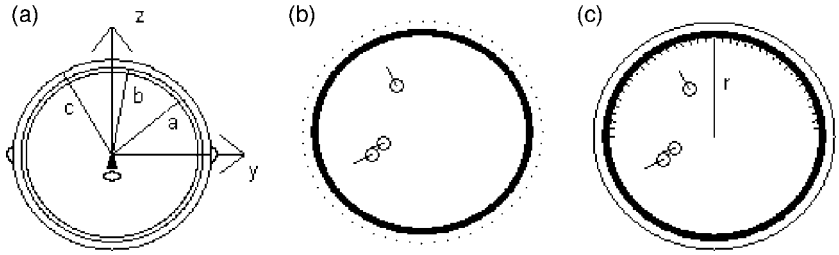

Figure 1. Three-concentric-sphere head model. (a) The head volume conductor model, where $a = 0.87$ (skull inner surface), $b = 0.92$ (skull outer surface) and $c = 1.0$ (scalp surface); the ear, nose and mouth are shown. (b) The approximate source potential model where the outset layer was removed; the three short bars illustrate the inside neural activities. (c) The equivalent dipole layer model where the radial dipoles on the layer are shown by short lines, the layer located at $r = 0.82$.

spatial or topographical features provide an access to the detection of focal EEG phenomena that have a relationship to focal pathology (Niedermeyer and Lopes da Siva 1999) or to localize brain function in cognitive science (Gevins *et al* 1999). A few approaches have been developed to construct an invasive high-resolution imaging map, which has been increasingly used in recent years. Here we classify them into two categories according to the location of the imaging surface: scalp surface or cortical surface based mapping.

The cortical surface based imaging techniques include the cortical surface potential (Sidman *et al* 1992), equivalent charge layer (ECL) (Yao 1996, 2003), equivalent dipole layer (EDL) (Freeman 1980, He *et al* 2002) and source potential (SP) (Yao 2001b). They are all reference-free, and each of them has a higher spatial resolution than the scalp potential map; however, they are all based on a detailed head volume conductor model including the boundaries and conductivities.

The scalp surface based mapping techniques include the scalp surface potential map recorded with a reference such as the average (Offner 1950), the scalp Laplacian (SL) (Hjorth 1975) and body surface charge model (He *et al* 1995). A scalp surface potential map suffers from the effect of reference and low spatial resolution. The extensively studied SL is of the highest spatial resolution but is difficult to estimate (Yao 2002a). The body surface charge model was based on a known Laplacian (He *et al* 1995) thus greatly limiting its practical feasibility because Laplacian measurement is more difficult than the potential recordings (Geselowitz and Ferrara 1999). To have an objective and high spatial resolution EEG map is the major goal of the researches in recent years.

In this work, we will provide a way to estimate the scalp ECL from the existing scalp potential recordings, and provide theoretical analysis and numerical comparison among the scalp ECL, SL and various scalp potentials with different references such as average (Offner 1950) and infinity (Yao 2001a), and an approximate source potential (aSP) which is produced by sources in the brain in a head model with the outset layer removed (figure 1(b)). The details of their physical model and mathematical relations are given in section 2, the method for getting these quantities is given in section 3 and application to EEG alpha (8–12 Hz) data of one male adult volunteer with his eyes closed is given in section 4. Finally in section 5 a conclusion and some discussions are included .

For convenience of reading, the main abbreviations are listed here: ECL, equivalent charge layer; SL, scalp Laplacian; EDL, equivalent dipole layer; SP, source potential; aSP, approximate source potential; EST, equivalent source technique; CC, correlation coefficient.

2. Forward solution

2.1. Potential produced by a dipole in a three-concentric-sphere head model

In this paper, the three-concentric-sphere head model (Rush and Driscoll 1969) is used as the head model. It is illustrated in figure 1(a), where the normalized radii are $a = 0.87$, $b = 0.92$ and $c = 1.0$, and normalized conductivities are $\delta_{1(r<a)} = \delta_{3(r>b)} = 1.0$, $\delta_{2(a<r<b)} = 0.0125$. In this model, with the spherical coordinate origin at the centre, it can be proved that the potential of a field point $\vec{r}(r, \theta, \varphi)$ produced by a dipole with moment $\vec{P}(P_r, P_\theta, P_\varphi)$ and position $\vec{r}_0(r_0, \theta_0, \varphi_0)$ may be expressed as (Yao 2000)

$$v(\vec{r}; \vec{r}_0) = \sum_{n,m} \frac{1}{r^{n+1}} \left(G_n^m(i; \vec{r}_0; \vec{P}) \cos m\varphi + H_n^m(i; \vec{r}_0; \vec{P}) \sin m\varphi \right) P_n^m(\cos\theta) \tag{1}$$

where

$$G_n^m(i; \vec{r}_0; \vec{P}) = K_n(i) g_n^m(\vec{r}_0; \vec{P}), \qquad H_n^m(i; \vec{r}_0; \vec{P}) = K_n(i) h_n^m(\vec{r}_0; \vec{P})$$
$$i = 1, \quad r \leqslant a; \qquad i = 2, \quad a \leqslant r \leqslant b; \qquad i = 3, \quad b \leqslant r \leqslant c. \tag{2}$$

And $\left(g_n^m(\vec{r}_0; \vec{P}), h_n^m(\vec{r}_0; \vec{P})\right)$ are the spherical harmonic spectra (SHS) coefficients of the dipole in an infinite medium, i.e. the strength coefficients of the equivalent multi-poles at the origin which produce the same potential as the actual potential of the real source. The $\left(g_n^m, h_n^m\right)$ may simply be noted in a complex as follows:

$$g_n^m + \mathrm{j} h_n^m = \frac{r_0^{n-1}}{4\pi\delta_1}(2 - \delta_{m0}) \frac{(n-m)!}{(n+m)!} \left(n P_r P_n^m(\cos\theta_0) + \frac{m P_\varphi}{\sin\theta_0} P_n^m(\cos\theta_0)\, \mathrm{e}^{\mathrm{j}\pi/2} \right.$$
$$\left. - \frac{P_\theta}{2}\left((n-m+1)(n+m) P_n^{m-1}(\cos\theta_0) - P_n^{m+1}(\cos\theta_0)\right) \right) \mathrm{e}^{\mathrm{j}m\varphi_0}, \qquad \mathrm{j} = \sqrt{-1}$$

where the radial coordinate $r_0 < a$ (i.e. the dipole is within the skull), $\delta_{m0} = 0$ $(m \neq 0)$, $\delta_{00} = 1$. P_n^m represents the associated Legendre function. $K_n(i)$ is a coefficient determined by the parameters of the head volume conductor model. On the scalp surface ($i = 3$, $r = c = 1.0$), we have (Yao 2000)

$$K_n(3) = \frac{(2n+1)(b^{2n+1} + \gamma)}{n(1-s)a^{2n+1} + \gamma(n + s(n+1))} \frac{n+1}{(n+1)b^{2n+1} + nc^{2n+1}} (c^{2n+1} + \chi) \tag{3}$$

where

$$s = \frac{\delta_2}{\delta_1} = \frac{\delta_2}{\delta_3}, \qquad f = b/c, \qquad \chi = \frac{n}{n+1} c^{2n+1}, \qquad \gamma = \frac{\alpha}{\beta}$$
$$\alpha = f^{2n+1}(1-s) - 1 - \frac{ns}{1+n}, \qquad \beta = f^{-(2n+1)}(1-s) - 1 - \frac{n+1}{n} s.$$

The potential calculated by equations (1)–(3) is referenced at infinity. $K_n(i)$ is a spatial filter. For practice, the scalp recordings must have a physical reference, such as an earlobe, or linked ears, or the average at each moment. For average reference, we have (Offner 1950)

$$v_a = v - Ta, \qquad a = \mathrm{mean}(v) \tag{4}$$

where T is a column vector with each of its elements unity. Here the lost average 'a' is unknown in general. However, as both v and v_a are produced by the same actual sources it gives us a chance to reconstruct v from the recording v_a as shown in Yao (2001a).

2.2. Source potential in a simplified head model

If a source is in an infinite volume conductor head model, the potential is defined as source potential (SP) (Yao 2001b), it is represented by equation (1) where no effect of the head model spatial filter is included, or say we have a spatial filter (Yao 2000)

$$K_n(\mathrm{SP}) = K_n(0) = 1 = K_n(3)/K_n(3). \tag{5}$$

Apparently, SP is head-model-free, and if we can reconstruct it from the scalp recordings, it will be a good imaging quantity (Yao 2001b). The last step in equation (5) shows us the way to reconstruct SP by an inverse spatial filter $1/K_n(3)$ acting on the scalp surface recordings. It is clear that a precise reconstruction needs the detail of the head model which is impossible for a practical case. For example, we may use a three-concentric-sphere head model or a MRI image-based head model; however, neither of them are the precise head model (various errors exist in the boundary and conductivity parameters), so the reconstructed SP is practically an approximate estimate of the actual SP.

In this work, we consider a feasible application of SP. Suppose we know the shape and the conductivity of the scalp layer, then we may reconstruct a potential without the scalp surface boundary by assuming the outspace with the same conductivity as the scalp layer, as shown in figure 1(b). For this case, the potential at the location of the scalp surface produced by the actual sources is free of the scalp–air boundary effect; we call this potential aSP.

Suppose the potential produced by a dipole in the model shown in figure 1(b) is

$$v_i(\vec{r};\vec{r}_0) = \sum_{n,m} \frac{1}{r^{n+1}}\left(E_n^m(\vec{r}_0;\vec{P})\cos m\varphi + F_n^m(\vec{r}_0;\vec{P})\sin m\varphi\right)P_n^m(\cos\theta), \quad r > b \tag{6}$$

where $E_n^m(\vec{r}_0;\vec{P})$ and $F_n^m(\vec{r}_0;\vec{P})$ are the SHSs of the dipole in the model shown in figure 1(b), then according to the air–scalp boundary condition, we should have

$$\frac{\partial v}{\partial r} = 0 \tag{7}$$

where v is a solution of the Laplace equation and v_i plus a variable reflects the effect of the air–scalp boundary; it is easy to show that the following v satisfies all these requirements (Frank 1952):

$$v(\vec{r};\vec{r}_0) = \sum_{n,m} \frac{1}{r^{n+1}}\frac{2n+1}{n}\left(E_n^m(\vec{r}_0;\vec{P})\cos m\varphi + F_n^m(\vec{r}_0;\vec{P})\sin m\varphi\right)P_n^m(\cos\theta), \tag{8}$$

while the potential should be the same as that represented by equation (1), so we have

$$\begin{aligned} E_n^m &= \frac{n}{2n+1}G_n^m = Q_n(\mathrm{aSP})K_n(3)g_n^m = K_n(\mathrm{aSP})g_n^m, \\ F_n^m &= \frac{n}{2n+1}H_n^m = Q_n(\mathrm{aSP})K_n(3)h_n^m = K_n(\mathrm{aSP})h_n^m \end{aligned} \tag{9}$$

where the spatial filter of aSP is

$$K_n(\mathrm{aSP}) = Q_n(\mathrm{aSP})K_n(3), \qquad Q_n(\mathrm{aSP}) = \frac{n}{2n+1}. \tag{10}$$

2.3. Scalp Laplacian

It is well known that SL may be characterized by a spatial filter (Yao 2000)

$$K_n(\mathrm{SL}) = Q_n(\mathrm{SL})K_n(3), \qquad Q_n(\mathrm{SL}) = -\frac{(n+1)n}{c^2}. \tag{11}$$

Based on equation (11), a negative SL corresponds to a positive scalp potential, and in the literature, the displayed SL is actually the negative SL. In this paper, we display SL directly.

2.4. Scalp equivalent dipole layer

It has been shown that the strength of EDL is proportional to the surface potential produced by the actual sources inside the surface with outside conductivity being zero (figures 1(a) and (c)) and that the boundary condition equation (7) is satisfied (Yao 2000, Yao and He 2003). So we have the spatial filter of the scalp EDL

$$K_n(\mathrm{EDL}) = \delta_3 K_n(3). \tag{12}$$

In other words, we may have the spatial filter of the scalp EDL by introducing the spatial filter $Q_n(d)$ (Yao 2000, 2003) to the spatial spectra in equation (6)

$$K_n(\mathrm{EDL}) = Q_n(d)K_n(\mathrm{aSP}) = \delta_3 K_n(3), \qquad Q_n(d) = \delta_3 \frac{2n+1}{n}. \tag{13}$$

Equation (11) means that the scalp EDL provides no more information than the scalp potential.

2.5. Scalp equivalent charge layer

It has been shown that the strength of ECL is the normal current of the layer when the outside is filled with a perfect conductor (Yao 2000, Yao and He 2003). Suppose we have potential produced by a dipole in the model shown in figure 1(c) characterized by equation (6), then we may get the scalp ECL on the location of the scalp surface by introducing the spatial filter $Q_n(q)$ (Yao 2000, 2003) to the spatial spectra in equation (6)

$$K_n(\mathrm{ECL}) = Q_n(q)K_n(\mathrm{aSP}) = Q_n(q)Q_n(\mathrm{aSP})K_n(3), \qquad Q_n(q) = \delta_3 \frac{2n+1}{c}. \tag{14}$$

Equation (14) provides us a chance to derive the scalp ECL from the scalp recordings by modifying the spatial filter from $K_n(3)$ to K_n (ECL).

2.6. Simulation of spatial filters

Figure 2 shows the spatial filters. The change in the normalized values with the increase in degree n is different for different filters; the scalp potential (also EDL) and aSP show a steep decrease, and aSP has a relatively smoother change thus implying a higher spatial resolution (Yao 2001b). SL and ECL show an increase, thus they will produce a higher spatial resolution map than the scalp potential. However, the amplification of high spatial frequency components also may amplify various wide-spectra noises (see figures 7 and 8). Besides, as 'a' is a constant in equation (4), the SHSs of v and v_a are the same, thus only the SHSs of v are shown in figures 3 and 7.

2.7. Summary

As shown above, for a given dipole including its moment and location, we have its spherical harmonic spectra coefficients $\left(g_n^m(\vec{r}_0;\vec{P}), h_n^m(\vec{r}_0;\vec{P})\right)$; then we may get the various variables by using different spatial filters. By $K_n(3)$ we get the scalp potential with reference at infinity; further by equation (4) we get the scalp potential with reference at average. By K_n(aSP), K_n(SL), K_n(EDL), K_n(ECL), we get aSP, SL, scalp EDL and ECL, respectively. In the literature, body surface ECL was introduced in electrocardiography studies, and it was based on knowing the Laplacian, which is more difficult to estimate in practice (He *et al* 1995, Geselowitz and Ferrara 1999). Here we introduce the scalp ECL based on the practical scalp potential recordings thus making it really feasible in practice.

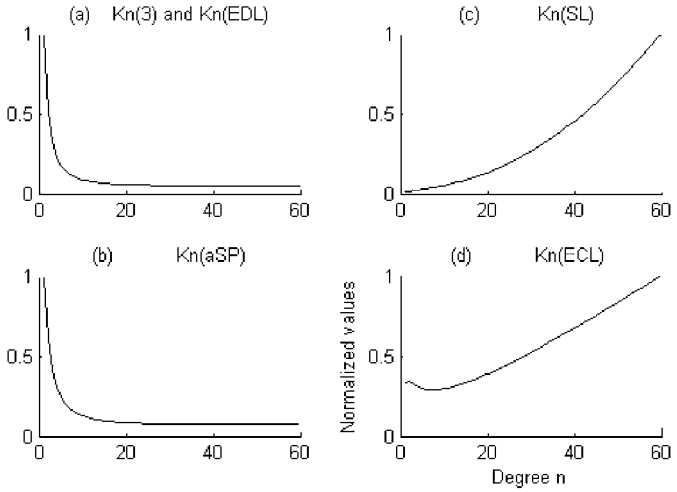

Figure 2. Normalized values versus degree n of the spatial filters. The horizontal axis is the degree n and the vertical axis is the normalized value of the spatial filters. (a) $K_n(3)$ is the filter of the three-concentric-sphere head model, and it is also the filter of the equivalent dipole layer K_n(EDL). (b) K_n(aSP) is the spatial filter of the volume conductor shown in figure 1(b). (c) K_n(SL) is the spatial filter of the scalp Laplacian. (d) K_n(ECL) is the spatial filter of the scalp surface equivalent charge layer.

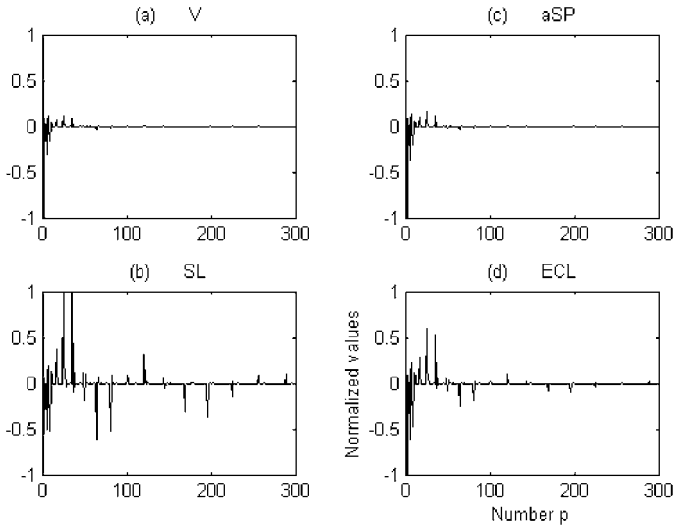

Figure 3. Normalized values of the SHS coefficients versus the order number p. The horizontal axis is the order number p of SHSs. The values of the SHS coefficients are the results of the spatial filters multiplying (g_n^m, h_n^m) and ordered in $p = 1$ ($n = 1$, $m = 0$), $p = 2$ ($n = 1$, $m = 1$), $p = 3$ ($n = 2$, $m = 0$), $p = 4$ ($n = 2$, $m = 1$) and so on. (a) The SHSs of the scalp potential with reference at infinity; (b), (c) and (d) the SHSs of SL, aSP and ECL, respectively.

3. Inversion solution

The above results show the way from known sources to the various scalp imaging quantities in a forward way. In practice, we do not know the sources, we need to get these imaging

variables from the only available scalp recordings with a reference, for example, the average reference (practical average reference, or re-referenced to average after recording with a scalp point such as an earlobe), the v_a in equation (4). As we know, there is no direct way to get the above variables except SL which may be approximately estimated by a direct derivative of the scalp recordings (Hjorth 1975). In this work, we use the equivalent source technique (EST) to complete the transform from the known scalp recordings to the desired variables. As EST has been extensively evaluated in the literature (Yao 1996, 2003, Yao *et al* 2001, Yao and He 2003), we just give a simple illustation as follows.

3.1. Equivalent source technique

In general, if a source configuration produces the same potential as an actual source in a supposed space, the former is the equivlaent source of the latter for the supposed space. Mathematically, any sources inside a closed layer may have an equivalent dipole or charge source layer on the layer surface (EDL or ECL) (Yao 2003, Yao and He 2003), or an equivalent series of multipoles at the origin of the coordinate system (the spherical harmonic expansion) (Yao 2000). For EDL, the discrete dipoles are oriented normal to the layer surface (Yao *et al* 2001).

As the number, positions, orientations (dipoles) and strengths of actual sources are unknown in general, the EEG inverse is very difficult. However, by EST, we may first assume the locations, orientations (dipoles) and number of a discrete approximate equivalent source layer (EDL or ECL), such as on the cortical surface which encloses all the actual sources inside; then the ECL or EDL reconstruction is much simpler than the actual source inversion. After we get ECL or EDL, we get the above imaging variables from the estimated equivalent sources instead of the unkown actual sources by the same forward calculation as shown above.

The discrete EDL model shown in figure 1(c) is the same as that used in Yao *et al* (2001); the mathematical model is

$$v(\vec{r}_j) = \sum_{i=0}^{I} s_i v(\vec{r}_j; \vec{r}(i)), \qquad j = 1, \ldots, M \tag{15}$$

where I is the number of equivalent sources; $v(\vec{r}_j, \vec{r}(i))$ is represented by equations (1)–(3), which is the transfer function from a unit radial dipole source located at $\vec{r}(i)(r(i), \theta(i), \varphi(i))$ to a measurement electrode position $\vec{r}_j(r_j, \theta_j, \varphi_j)$. M is the number of electrodes. On the basis of the recordings $v(\vec{e}_j)$ derived from the scalp electrodes $\vec{r}_j = \vec{e}_j$ $(r_j = 1, \theta_j, \varphi_j)$, $j = 1, \ldots, M$, we have

$$v(\vec{e}_j) = \sum_{i=0}^{I} s_i v(\vec{e}_j; \vec{r}(i)) \quad j = 1, \ldots, M \tag{16}$$

where both $v(\vec{e}_j)$, the scalp recordings, and $v(\vec{e}_j; \vec{r}(i))$, the potential produced by a unit normal dipole, are known; the strength s_i of EDL may be found by a linear inversion of equation (16).

The linear inversion is implemented by a direct inversion of equation (16) with the singular value decomposition (Yao *et al* 2001, Yao 2003). In this work, EDL is assumed to exist at $r = 0.82$, and is composed of $I = 2560$ discrete radial dipoles uniformly distributed on the upper hemispheric equivalent layer surface. The singular values are terminated at 123 because only 123 channels of the total 124 channels are independent when an average reference is used (Yao 2001a), and the ratio of the 123rd to 1st singular values is 0.0053, which is not a serious singular case.

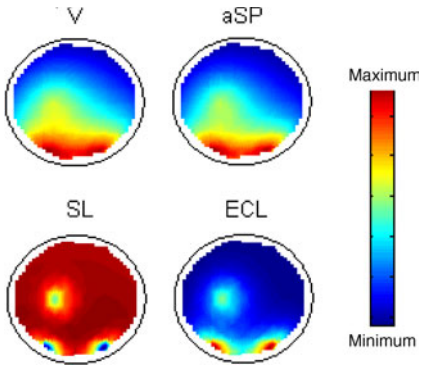

Figure 4. Forward maps. V: the scalp potential v with reference at infinity; it is also the map of v_a and EDL as EDL is proportional to v, and the difference between v and v_a is only a constant; aSP: the approximate source potential map on the scalp surface position of the model shown in figure 1(b); SL: scalp Laplacian; ECL: the scalp equivalent charge layer. The maps are displayed after the values being normalized by the absolute maximum value of each sub-figure, thus the colour bar just shows the relative value, and this is the case for all the following maps in figures 5, 6, 8, 10 and 11 where the colour bars are omitted.

3.2. Simulation test

In the simulation calculations, the midpoint between the left and right preauricular points is defined as the Cartesian coordinate origin. The axis directed away from the origin towards the left preauricular point is defined as the $+y$ axis, and that from the origin to the nasion is the $+x$ axis. The $+z$ axis is defined as the axis that is perpendicular to both these axes and directed from the origin to the vertex. The electrode number $M = 124$, the coordinates of the electrodes are the normalized standardization coordinates selected from the 10–5 extension of the International 10–20 electrode system (Oostenveld and Praamstra 2001) which was utilized in the collection of the following real data.

3.2.1. Forward simulation. Suppose that there are three dipoles in the volume conductor model, the locations of which in Cartesian coordinate are respectively $(x, y, z) = (-0.6, -0.3, 0.3)$, $(-0.6, 0.3, 0.3)$ and $(0.0, 0.2, 0.7)$, and the corresponding moments in components of Cartesian coordinate axes are $(-0.816\,549, -0.408\,274, 0.408\,274)$, $(-0.816\,549, 0.408\,274, 0.408\,274)$ and $(0.000\,000, 0.137\,363, 0.480\,769)$, respectively. The former two are unit normal dipoles, and the third one is a half-unit normal dipole.

Figure 3 shows the normalized values of the SHS coefficients versus the order number. They are the results of the above spatial filters (figure 2) multiplying SHS of the actual sources $\left(g_n^m, h_n^m\right)$. It is clear that the content of high spatial frequency components is ordered in the way of SL>ECL>aSP>V. Figure 4 shows the forward maps of the sources, where we see the spatial resolution order also is SL>ECL>aSP>V, consistent with the information on the spatial filters shown in figures 2 and 3.

3.2.2. Inverse simulation. Figure 5 shows the reconstructed equivalent source distribution on the cortical surface ($r = 0.82$). It is of much higher spatial resolution than the scalp potential map (figure 4(V)), and this is the rationale of the equivalent dipole layer imaging (He *et al* 2002). On the basis of the reconstructed equivalent sources, by the same forward calculation as above for the known sources, we may reconstruct SHS and scalp maps, and we found the results (figures omitted) are very similar to the forward situation shown in figure 4. The

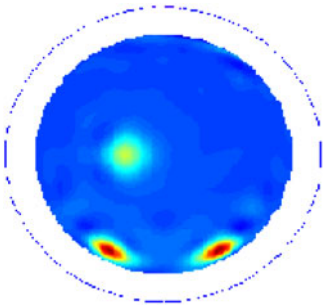

Figure 5. Distribution of the reconstructed equivalent dipole layer. The layer is on the surface with radius $r = 0.82$.

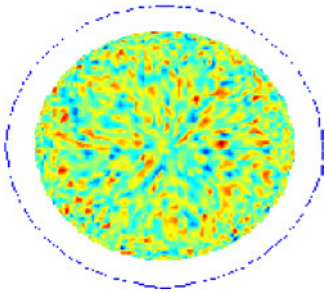

Figure 6. Noisy cortex neural activities. The values are random numbers generated by Matlab. The mean is 0.0037 and the standard deviation is 1.0188.

correlation coefficient (CC) between the direct forward values (figure 4) and the reconstructed values (omitted) are all 1.0 except SL which is 0.9967.

Besides, comparing figures 4 and 5, we see that the scalp ECL and SL may even have a higher spatial resolution than the cortical EDL does.

3.2.3. Noise test. As the calculation from the cortical neural activities to the scalp variables is a linear calculation, we may simulate the actual neural activities (here the above three sources), and noisy cortical sources independently and mix them in various ratios.

By running a random number generator in Matlab, we get the strengths of the same size random normal dipole sources on the same layer $r = 0.82$ as shown in figure 6, where the mean is 0.0037 and the standard deviation is 1.0188. Figures 7 and 8 show the corresponding SHSs and maps on the scalp surface. When comparing figure 8 with figure 6, many high spatial frequency components are filtered out by the head model especially in scalp potential (V) with reference at infinity and aSP (looking at $K_n(3)$ and K_n(aSP) in figure 2). However, if comparing with figures 3 and 4, many more high spatial frequency components are in figures 7 and 8 especially in SL and ECL, this fact means SL and ECL are much more sensitive to noise of wide spectra, especially SL.

Figure 9 shows the effect of noisy cortical activities where the horizontal axis shows the ratio of the absolute maximum value in figure 5 to that in figure 6. CC is between the scalp variables produced by cortex activities in figure 5 as shown in figure 4 and the scalp variables produced by cortex activities in figure 5 mix with those in figure 6 in different ratios. It clearly shows the relative sensitivity to the noise is ordered as SL>ECL>aSP>V, and this is consistent with the characteristics of the spatial filters shown in figure 2.

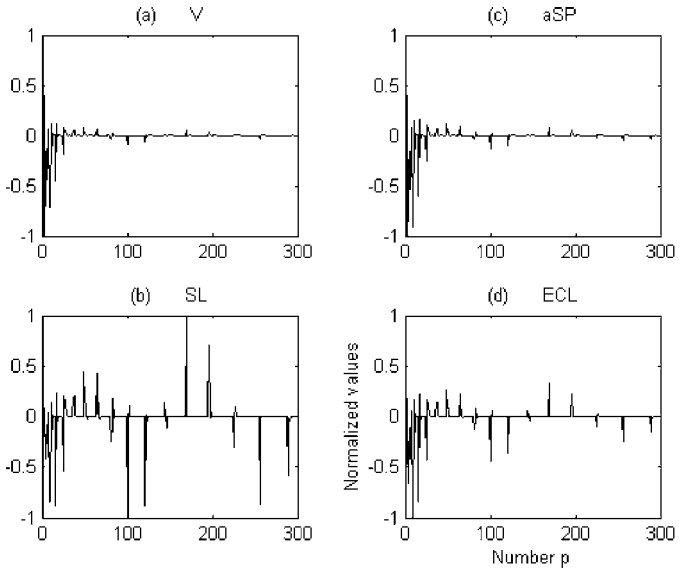

Figure 7. Normalized values of the SHS coefficients versus the order number p. The horizontal axis is the order number p of SHSs. They are the results of the spatial filters multiplying (g_n^m, h_n^m) and ordered as $p = 1$ $(n = 1, m = 0)$, $p = 2$ $(n = 1, m = 1)$, $p = 3$ $(n = 2, m = 0)$, $p = 4$ $(n = 2, m = 1)$ and so on. (a) The SHSs of the scalp potential with reference at infinity; (b), (c) and (d) the SHSs of SL, aSP and ECL, respectively.

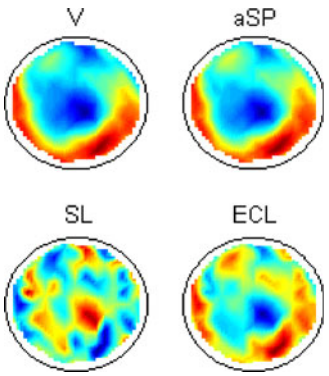

Figure 8. Forward maps of the noisy cortex activities. V: the scalp potential v with reference at infinity; it is also the map of v_a and EDL as EDL is proportional to v, and the difference between v and v_a is only a constant; aSP: the approximate source potential map on scalp surface position; SL: scalp Laplacian; ECL: the scalp equivalent charge layer.

Figure 10 shows the scalp variables when the mixture ratio is 1.5; it shows that ECL is a little less sensitive than SL to the noise.

4. Real EEG data test

One male adult volunteer (HM), about 25 years, was recruited. Informed consent was obtained from the subject prior to the study. The study was approved by the Local Ethics Committee and made in accordance with the Helsinki declaration. The experiment was performed in a

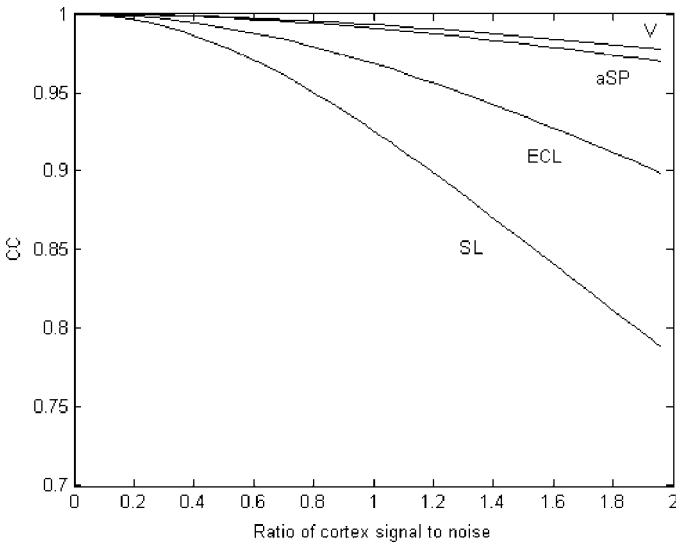

Figure 9. Effect of noise activities on scalp variables. The horizontal axis shows the ratio of the absolute maximum value in figure 5 to that in figure 6. CC is between the scalp variables, shown in figure 4, produced by cortex activities in figure 5 and the scalp variables produced by cortex activities in figure 5 plus figure 6 in different ratios.

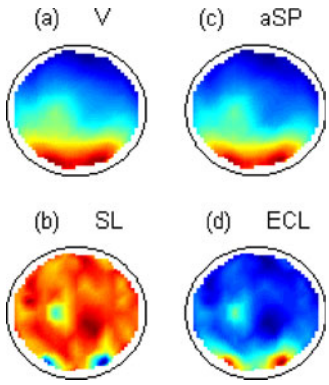

Figure 10. Effect of noise activities on scalp mapping. They are the scalp variables produced by assumed meaningful cortex activities in figure 5 plus noisy cortex activities in figure 6 at a ratio 1.5 of the absolute maximum value in figure 5 (signal) to that in figure 6 (noise).

quiet air-conditioned (20–21 °C) laboratory with soft natural light. The subject was requested to relax and sit in a comfortable chair with his eyes closed. The EEG was recorded from 128 surface electrodes (including two EOG channels) mounted on the scalp using a standard EEG-cap (ANT, Enschede, The Netherlands). The EEG epochs of 1 min were sampled at 512 Hz, and the electrode impedance was below 10 kW. The on-line reference was the left mastoid, and the data were re-referenced off-line to average reference for further analysis as shown above to get the other imaging variables.

The scalp potentials V were segmented to epochs of 2 s, and epochs free of muscle, EOG, and movement artefacts were visually selected off-line. Here, as the EEG data are related to spontaneous neural activities, we calculate the power maps of all the variables in the alpha

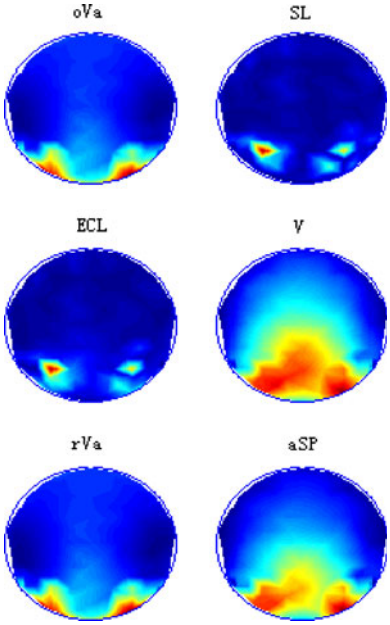

Figure 11. Alpha power mapping of a subject with eyes closed. The original recording with average reference is oV_a; SL: the scalp Laplacian; ECL: the scalp equivalent charge layer; V: the reconstructed potential with reference at infinity; rVa: the reconstructed recording with average reference (from the reconstructed V); aSP: the reconstructed approximate source potential.

frequency band (8–12 Hz) by FFT (Welch's method in Matlab). Figure 11 shows the results; it is clear that SL and ECL give us much higher spatial resolution maps than all the other various potential maps.

If we check CCs among these variables, it is 0.9856 between ECL and SL, which means the two techniques provide similar high-resolution results. CC is 1.0 between the original scalp recordings with average reference (oV_a) and the reconstructed recordings (rV_a) with average reference; this fact means the inverse is good. Besides, aSP shows a little higher spatial resolution than oV_a; the detectable difference (CC = 0.9938) between oV_a/rV_a and V means the average reference does introduce some changes of the power map, thus giving practical value of all the reference-free techniques: ECL, EDL(V), SL and aSP. All the results clearly support the basic fact that the main alpha activities are in the occipital area when the eyes are closed.

5. Conclusion and discussions

The above simulation and real data tests show that scalp surface ECL and SL may be two powerful techniques for mapping the underlying neural electric activities; they may even be superior to the cortical dipole layer mapping. The results also confirm that a scalp-potential-based ECL estimate is feasible and meaningful for practice. Meanwhile, aSP also provides a little higher spatial resolution than the scalp surface potential map. The power map of real spontaneous EEG alpha activities shows that the average reference may have a detectable effect on the map.

For the difference between ECL and SL, SL is approximately proportional to the cortical potential, and may therefore be interpreted as a spatial de-convolution of the scalp potential

(Nunez *et al* 1994). It was also shown that SL has some relation to the scalp current density (SCD) (Hjorth 1975, Yao 2002b), thus sometimes the two terms, SL and SCD, are assumed to be the same. However, in physics, SCD is not SL, and SL is also not the cortical potential; these facts mean SL does not have physical meaning in nature though it is a useful way to approximately estimate the physical quantities, SCD and cortical surface potential. Meanwhile, ECL has a clear equivalent physical model. The strength of ECL is the strength of the normal current passing the layer where ECL is located when the outside is filled with a perfect conductor (Yao 2000, Yao and He 2003).

In this work, we use the equivalent dipole layer technique to get the scalp ECL and SL etc; we may use a charge layer (Yao 2003) as the intermediate step. Meanwhile, in the three-concentric-sphere head model used here, the ratio of brain to skull conductivity was 80, and it was a widely used ratio in the published literature. Recently, better-controlled experimental works suggested a factor closer to 15 (Oostendorp *et al* 2000) or 18 (Akhtari *et al* 2002), thus a different ratio may be chosen in the further application of the techniques developed here.

When compared with the cortical surface mapping, the variables used here on the scalp surface are more feasible because they do not need the detailed head model. For example, though we need to reconstruct the equivalent source layer with a head model, in general, we do not need to know the detailed correct model, because any inaccuracy may be integrated into the reconstructed equivalent dipole layer. In other words, a very accurate head model may help us to get a more accurate equivalent dipole layer when compared with the actual equivalent dipole layer as the theory predicted (Yao and He 2003), and a coarse head model will make us get a changed equivalent dipole layer but both cases will produce the same scalp potential as they would produce almost the same other scalp variables as revealed in our previous test (Yao 2001a). These facts mean that the scalp surface based techniques are more head model independent, thus making them more feasible in practice.

Acknowledgments

This work is supported by the NSFC.90208003 and the 973 Project No 2003CB716106, the Key Project of Science and Technology of MOE PRC (02065), Doctor training Fund of MOE PRC and TRAPOYT, and funding from the Danish National Research Foundation, the Sichuan Youth Research funding of PRC, the International Centre for Biomedical Research of Denmark, The Aalborg University visiting scientist Awards, Denmark.

References

Akhtari M *et al* 2002 Conductivities of three-layer live human skull *Brain Topogr.* **14** 151–67

Frank E 1952 Electric potential produced by two point current sources in a homogeneous conducting sphere *J. Appl. Phys.* **23** 1225–8

Freeman W 1980 Use of spatial de-convolution to compensate for distortion of EEG by volume conductor *IEEE Trans. Biomed. Eng.* **37** 421–9

Geselowitz D B and Ferrara J E 1999 Is accuracy recording of the ECG surface Lapacian feasible? *IEEE Trans. Biomed. Eng.* **46** 377–81

Gevins A, Smith M E, McEvoy L K, Leong H and Le J 1999 Electroencephalographic imaging of higher brain function *Phil. Trans. R. Soc.* B **354** 1125–33

He B, Chernyak Y B and Cohen R J 1995 An equivalent body surface charge model representative three-dimensional bioelectrical activity *IEEE Trans. Biomed. Eng.* **42** 637–46

He B, Yao D and Lian J 2002 High-resolution EEG: on the cortical equivalent dipole layer imaging *Clin. Neurophysiol.* **113** 227–35

Hjorth B 1975 An online transformation of EEG scalp potentials into orthogonal source derivations *Electroencephalogr. Clin. Neurophysiol.* **39** 526–30

Niedermeyer E and Lopes da Siva F 1999 *Electroencephalography Basic Principles, Clinical Applications and Related Fields* 4th edn (Baltimore, MD: Williams and Wilkins)

Nunez P L, Silberstein R B, Cadusch P J, Wijesinghe R S, Westdorp A F and Srinivasan R 1994 A theoretical and experimental study of high resolution EEG based on surface Laplacian and cortical imaging *Electroencephalogr. Clin. Neurophysiol.* **90** 40–57

Offner F F 1950 The EEG as potential mapping: the value of the average monopolar reference *EEG Clin. Neurophysiol.* **2** 215–6

Oostendorp T F, Delbeke J and Stegeman D F 2000 The conductivity of the human skull: results of *in vivo* and *in vitro* measurements *IEEE Trans. Biomed. Eng.* **47** 1487–92

Oostenveld R and Praamstra P 2001 The 5% electrode system for high-resolution EEG and ERP measurements. *Clin. Neurophysiol.* **112** 713–9

Rush S and Driscoll D A 1969 EEG electrode sensitivity—an application of reciprocity *IEEE Trans. Biomed. Eng.* **16** 15–22

Sidman R D, Vincent D J, Smith D B and Lee L 1992 Experimental tests of the cortical imaging technique *IEEE Trans. Biomed. Eng.* **39** 437–44

Yao D 1996 The equivalent source technique and cortical imaging *Electroencephalogr. Clin. Neurophysiol.* **98** 478–83

Yao D 2000 High-resolution EEG mappings: a spherical harmonic spectra theory and simulation results *Clin. Neurophysiol.* **111** 81–92

Yao D 2001a A method to standardize a reference of scalp EEG recordings to a point at infinity *Physiol. Meas.* **22** 693–711

Yao D 2001b Source potential mapping: a new modality to image the neural electrical activities *Phys. Med. Biol.* **46** 3177–89

Yao D 2002a High-resolution EEG mapping: a radial-basis function based approach to the scalp Laplacian estimate *Clin. Neurophysiol.* **113** 956–67

Yao D 2002b The theoretical relation of sclap Laplacian and scalp current density of a spherical shell head model *Phys. Med. Biol.* **47** 2179–85

Yao D 2003 High-resolution EEG mapping: an equivalent charge-layer approach *Phys. Med. Biol.* **48** 1997–2011

Yao D and He B 2003 Equivalent physical models and formulation of equivalent source layer in high-resolution EEG imaging *Phys. Med. Biol.* **48** 3475–83

Yao D, Zhou Y, Zeng M, Fan S, Lian J, Wu D, Ao X, Chen L and He B 2001 A study on equivalent source techniques of high-resolution EEG imaging *Phys. Med. Biol.* **46** 2255–66